ORIGINAL PAPER

Newly isolated sporopollenin microcages from *Cedrus libani* and *Pinus nigra* as carrier for Oxaliplatin; xCELLigence RTCA-based release assay

Muhammad Mujtaba[1] [ORCID] · **Bahar Akyuz Yilmaz[2]** · **Demet Cansaran-Duman[1]** · **Lalehan Akyuz[3]** · **Sevcan Yangın[1]** · **Murat Kaya[2]** · **Talip Çeter[4]** · **Khalid Mahmood Khawar[5]**

Abstract

Sporopollenin-mediated control drug delivery has been studied extensively owing to its desirable physicochemical and biological properties. Herein, sporopollenin was successfully extracted from *C. libani* and *P. nigra* pollens followed by loading of a commonly known anticancer drug Oxaliplatin. Drug loading and physicochemical features were confirmed by using light microscopy, FT-IR, SEM and TGA. For the first-time, real-time cell analyzer system xCELLigence was employed to record the Oxaliplatin loaded sporopollenin-mediated cell death (CaCo-2 and Vero cells) in real time. Both the release assays confirmed the slow release of oxaliplatin from sporopollenin for around 40–45 h. The expression of MYC and *FOXO-3* genes has been significantly increased in CaCo2 cell and decreased non-cancerous Vero cell confirming the fact that sporopollenin-mediated control release of oxaliplatin is promoting apoptosis cell death preventing the spread of negative effects on nearby healthy cells. All the results suggested that *C. libani* and *P. nigra* can be suitable candidates for the slow delivery of drugs.

Keywords xCELLigence · Real-time cell analyzer · Controlled-drug release · Sporopollenin

✉ Muhammad Mujtaba
muhammadmujtaba443@gmail.com; mujtaba@ankara.edu.tr

[1] Institute of Biotechnology, Ankara University, 06110 Ankara, Turkey

[2] Department of Biotechnology and Molecular Biology, Faculty of Science and Letters, Aksaray University, 68100 Aksaray, Turkey

[3] Department of Chemistry Technology, Technical Vocational School, Aksaray University, 68100 Aksaray, Turkey

[4] Department of Biology, Faculty of Arts and Sciences, Kastamonu University, 37100 Kastamonu, Turkey

[5] Department of Field Crops, Faculty of Agriculture, Ankara University, 06100 Ankara, Turkey

Ⓐ Springer

Introduction

Designing and production of drug carrier systems for slow and targeted release to prevent the premature burst release of the content in the bloodstream represents an ever-evolving research and application area in biomedical science [1, 14, 40, 47]. In recent years with the advancements in nanotechnology, huge efforts have been made to design carrier systems exhibiting the desired structural and chemical properties [10, 18, 19]. Nano/micro-vehicles tested so far for the controlled release of anticancer drugs include liposomes, water-soluble polymers, dendrimers, vesicles [41], polymeric nanoparticles [16, 20, 21, 34], and some inorganic materials [5, 15, 17, 35]. All the tested drug carriers had their pros and cons. For example, the encapsulation capacity of liposomes and nanoparticles has been reported around 10% [31, 38, 48]. Besides, obtaining the nanocarriers with desired geometry and functional properties requires expensive processes in large time scales [7]. In this regard, the quest has been underway for producing alternative macro/nano/microcarriers which offer several properties such as non-toxic, non-reactive with load, economical, and biodegradable. In nature, a variety of biomaterials are already present which have the application capabilities in different fields. These natural materials have been evolved in much longer time scales, thus ensuring the fidelity and physicochemical properties of such materials. Among many examples, polen comes with excellent features such as excellent elasticity, size uniformity, homogeneity in pore sizes, physical and chemically resistance, UV shielding ability, and antioxidant ability [11, 28].

Since the last decade, researchers have actively focused on the development and modification of plant pollen as a delivery vehicle for many active ingredients such as drugs [12, 24, 43], active compounds [27]. Considering the up-to-date research related to the utilization of sporopollenin for the controlled delivery of anticancer drugs, researchers are conducting the in vitro release assays using different buffer solutions to simulate the intestine and stomach environment and to investigate the release effect of the drug from carrier [3, 13, 29]. However, the release assays have not been conducted using novel real-time cell analyzer tools such as xCELLigence to get a more accurate perspective of the controlled release in cancer cells. To bridge this gap in the literature, besides the conventional release assay (simulated pH systems), the current study was mainly designed to get an inclusive insight of the sporopollenin-based release in cancer cells by using a recently developed tool known as a real-time cell analyzer. Most of the anticancer drugs exhibit problems like poor water solubility, rapid blood clearance, low tumor selectivity, and severe side effects for healthy tissues [31]. For this purpose, several delivery systems have been tested for the controlled release of anticancer drugs. As is known that in apoptosis the cell dismantled in rather a controlled way from inside minimizing the damage and disruption to the surrounding healthy cells. The resulting debris is then removed through phagocytes [36]. While in necrosis the abrupt dismantling of cells releases the debris into the surrounding healthy cells [4]. Considering these facts, it is fathomable that the slow release of the therapeutic drug may have a direct link with cell apoptosis. In the current study, two reference genes i.e., *c-Myc* and *FOXO3* have been selected to assess the effect of sporopollenin-mediated slow release of

Oxaliplatin on cell death by apoptosis. *c-Myc* gene plays a regulatory role in cell proliferation and cellular metabolism by inducing apoptosis [26]. Another gene we selected in this study, *FOXO3*, promoting apoptosis through the expression of genes responsible for cell death [9]. Thus, by determining the level of expression of both genes, we have determined the possible relationship of sporopollenin to apoptosis.

In the current study, the sporopollenin of *C. libani* and *P. nigra* were tested as a control release vehicle for a common anticancer drug known as Oxaliplatin. Pinus and Cedrus belong to Pinaceae family. Around, 80 species of the Pinus genus that distributed from the Northern hemisphere to the Tropics [32]. There are five naturally grown species in our country. 10–20 m tall, evergreen trees with 2–3 or 5 needle leaves coming out of the shoots [33]. Male cones are located at the bottom of small, yellow, young shoots, and female cones are located green, close to the tip. *Pinus nigra* pollen is monad, heteropolar and bilateral symmetry. The pollen shape is equilateral oblates, pollen type vesiculate, bisaccate. *Cedrus libani* pollens are monad, heteropolar and bilateral symmetry. The pollen shape is an equatorially appearance oblate, pollen type vesiculate, bisaccate [2].

To the best of our knowledge, no study has been reported on the *C. libani* and *P. nigra* sporopollenin production and its utilization as a controlled-drug vehicle for Oxaliplatin and the effect of this slow release on cell death. Besides the conventional release measurement assay (simulated pH systems), the first-time real-time cell analyzer model (xCELLigence) has been employed to determine the slow release from sporopollenin in real time. Here, the sporopollenin production and drug loading were confirmed by using analytical tools such as light microscopy, SEM, FT-IR, and TGA. The release assays were conducted both in simulated pH solutions and cell culture (Caco-2 and Vero) using a real-time cell analyzer (xCELLigence). The effects of sporopollenin-mediated slow release of oxaliplatin over apoptosis was investigated. The cell apoptosis was analyzed using two reference genes with main roles in cell apoptosis known as *FOXO-3* and *c-MYC*.

Materials and methods

Pollen collection

In the current study, the pollens of *Cedrus libani* and *Pinus nigra* were collected in the year 2015 from the garden of Education Faculty and Vocational School of Kastamonu University, respectively. Male cones collected with vintage scissors were placed in clean paper bags and brought to the laboratory. It was then spread over clean papers and covered with paper to prevent contamination and allowed to dry at room temperature for 3 days. Drying male cones were shaken to shed pollen. The obtained pollens were sieved (having a pore diameter of 10 μm) to be free from dust and other unwanted particles. To obtain pure pollens, the remaining pollen was again passed through a sieve having a pore diameter of 100 μm to remove large particles. The purified pollen samples were stored in sealed falcon tubes at −20° for further experiments.

Chemicals

CH_3OH, $CHCl_3$, HCl, KCl, KH_2PO_4, NaCl, NaOH, and Na_2HPO_4 have been purchased from Sigma-Aldrich (St. Louis, Missouri, USA). PBS (phosphate buffer saline) buffer was prepared at pH 7.4 by using Na_2HPO_4, KH_2PO_4, NaCl, and KCl. Distilled water has been used at all experimental steps. DMEM (Sigma, UK), Penicillin/streptomycin (Sigma, UK), and non-essential amino acid (Gibco, Grand Island), Fetal Bovine Serum (Biological Industries, USA), and PBS (Biological Industries, USA).

Sporopollenin isolation

To obtain sporopollenin, the obtained pollens were treated with acid, base, and chloroform/methanol/water solution for demineralization, deproteinization and depigmentation. Briefly, for demineralization, 10 g of *C. libani* and *P. nigra* pollen were treated with 4 M HCl solution at 50° C for 2 h. Then, the samples were filtered by a Whatman filter paper with a pore size of 110 μm following by an extensive wash with distilled water until neutral pH. For deproteinization, the samples were incubated with 4M NaOH solution at 150° C for 6 h. Then, the treated samples were filtered using Whatman filter paper and extensively washed with distilled water until neutral pH. The demineralization and deproteinization treatments were repeated 4 times to ensure the complete removal of genetic and cellulosic materials inside the pollen. The acid and base-treated pollen samples were then allowed at room temperature for 1 h in chloroform/methanol/water solution (4: 2: 1/v: v: v). Finally, the samples of sporopollenin were thoroughly washed with distilled water and dried in the oven at 60° C for 48 h [24]. The samples were coded as Oxaliplatin drug (*OX*), *Pinus nigra* raw pollen (PN), *Pinus nigra* sporopollenin (*PN-SP*), Oxaliplatin loaded *Pinus nigra* sporopollenin (*PN-SP-OX*), *Cedrus libani* raw pollen (*CD*), *Cedrus libani* sporopollenin (*CD-SP*), Oxaliplatin loaded *Cedrus libani* Sporopollenin (*CD-SP-OX*).

Physicochemical analysis

FT-IR

The spectra of Oxaliplatin drug (*OX*), *Pinus nigra* raw pollen (PN), *Pinus nigra* sporopollenin (*PN-SP*), Oxaliplatin loaded *Pinus nigra* sporopollenin (*PN-SP-OX*), *Cedrus libani* raw pollen (*CD*), *Cedrus libani* sporopollenin (*CD-SP*), Oxaliplatin loaded *Cedrus libani* Sporopollenin (*CD-SP-OX*) were analyzed in the range of 4000-650 cm-1 using an FT-IR spectrometer (PerkinElmer 100, USA) under ambient conditions.

TGA

All samples were heated from 30 to 650 °C with a temperature change of 10 °C/min and their thermal stability, water, and ash content were determined. All the

thermograms were recorded with an EXSTAR S11 7300 (USA) instrument under the nitrogen atmosphere.

SEM

The drug, pollen, and sporopollenin samples were placed on aluminum stab with double side adhesive type, and it was covered with gold by Cressington, Sputter Coater 108 Auto Au–Pd Coating Machine at Kastamonu University Central Research Laboratory, under 40 mA for 30 s. SEM photos were taken with FEI-Quanta FEG 250 model scanning electron microscope.

Light microscopy

The sporopollenin production and drug loading were also confirmed by analyzing the samples under a LEICA DFC425 C light microscope. The samples were analyzed in ambient conditions using glass slid.

Loading of Oxaliplatin to sporopollenin via passive loading technique

Oxaliplatin was loaded onto *C. libani* and *P. nigra* sporopollenin by the passive loading technique used in our previous study [29]. Briefly, in the passive loading technique, 100 mg of Oxaliplatin was dissolved in 4 mL of distilled water with the aid of sonification for 10 min. Then, 200 mg of *C. libani* and *P. nigra* sporopollenin were added to this solution separately and the suspension was vortexed for 15 min. Each sporopollenin-Oxaliplatin solution was then incubated at 350 rpm using a thermo-shaker for 4 h and at 4 °C. The samples were then filtered with filter paper having a pore size of 110 μm and washed twice with 3 mL of distilled water. The drug-loaded sporopollenin samples were incubated at −80° C for 30 min. Finally, Oxaliplatin loaded sporopollenin were dried at room temperature for 24 h and then stored at −18° C for further experiments.

Encapsulation efficiency

Quantitative determination of Oxaliplatin loaded on *C. libani* and *P. nigra* sporopollenin was carried out by following previously reported methods with minor modifications [25]. Oxaliplatin was dissolved in different concentrations i.e., 5 μg/mL, 10 μg/mL, 15 μg/mL, 20 μg/mL and 25 μg/mL to obtain the calibration curve. The absorbance of these solutions was measured at 255 nm using a UV–vis spectrophotometer. To evaluate the drug loading efficiency of both sporopollenin samples, 10 mg of Oxaliplatin loaded *C. libani* and *P. nigra* samples were vortexed for 10 min by adding 3 mL of PBS. Then, the samples were filtered through a Whatman filter paper with a pore size of 110 μm. The clear solution was collected and measured at 255 nm using UV-spectrophotometer. The following equations are used to calculate the loading efficiency:

$$\text{Amount of drug (mg)} = (\text{Absorbance} \times \text{dilution factor})/(\text{Slope} \times 1000) \quad (1)$$

$$\text{Drug loading } (\%) = (\text{Amount of drug/Mass of drug-loaded sporopollenin}) \times 100 \quad (2)$$

$$\text{Drug loading efficiency } (\%) = (\text{Calculated drug loading/Theoretical drug loading}) \times 100 \quad (3)$$

In vitro release studies with Oxaliplatin loaded microcages

In vitro, drug release studies of Oxaliplatin loaded sporopollenin obtained using passive loading technique were performed using PBS (pH 7.4) buffer as simulated intestinal fluid. Briefly, 10 mg of drug-loaded sporopollenin were added separately to 5 mL of PBS buffer solution. Each solution was then transferred to dialysis bags and placed in 50 mL of PBS solution. The samples were then shaken in a water bath at 37 °C at 100 rpm for 120 h. Then, to calculate the amount of Oxaliplatin released from the sporopollenin contained in the dialysis bag into the PBS solution, 2 mL of PBS was drawn at 5th min, 15th min, 30th min, 1st, 2nd, 6th, 24th, 48th, 72nd, and 120th h time intervals. The same amount of fresh PBS buffer solution was added back to the medium for maintaining the volume. The amount of Oxaliplatin released into the medium was measured using a *UV–VIS* spectrophotometer at 255 nm. Besides, to control the release of free drug, 10 mg Oxaliplatin was added to the PBS solution and in vitro release studies were performed by following the above procedure.

The following equations were used to calculate the cumulative percent release of Oxaliplatin:

$$\text{Drug concentration } (\text{mg/mL}) = (\text{Absorbance} \times \text{Slope}) \pm \text{Intercept} \quad (4)$$

$$\text{Drug quantity (mg)} = (\text{Concentration} \times \text{dissolution bath volume}) \quad (5)$$

$$\text{Cumulative percent release } (\%) = (\text{volume of the sample withdrawn from media (mL)}/$$
$$\text{dissolution bath volume (mL)}) \times P(t-1) + Pt \quad (6)$$

Pt denotes the percentage release at time t, $P(t-1)$ is the percentage release previous to t.

Real-time release assay on cell lines

Cell culture

CaCo-2 and Vero cells were kindly provided by the Ministry of Health, Turkey Pharmaceuticals and Medical Devices Agency. CaCo-2 cancer cell was cultured in Dulbecco's modified Eagle's medium (DMEM, Gibco, Grand Island, NY, USA) supplemented with 1% penicillin/streptomycin (Gibco, Grand Island, NY, USA), 1% amino acid (Gibco, GrandIsland, NY, USA), 20% Fetal bovine serum

(Lonza, Verviers, Belgium), at 37 °C in a humidified atmosphere containing 5% CO_2. Vero, non-cancerous cell line, was cultured in DMEM (Gibco, Grand Island, NY, USA) supplemented with 10% Fetal bovine serum (Lonza, Verviers, Belgium), 1% penicillin/streptomycin (Gibco, Grand Island, NY, USA) in a 5% CO_2 humidified incubator at 37 °C.

Antiproliferative effect by sporopollenin-based control release (xCELLigence, RTCA)

The cell proliferation was also continuously monitored using the xCELLigence RTCA Instrument (xCELLigence RTCA, Roche, Germany) according to the manufacturer's instructions. CaCo-2 and Vero cells seeded at a density of 5×10^3 cells and 7×10^3 per well in 200 μl media containing 10% FBS in of 16 well E-plate (Roche Applied Science, Germany), respectively. After 24 h, drug-loaded sporopollenin of *P. nigra*, *C. libani* and pure Oxaliplatin (control) were added at different concentrations (at the range of 5–20 mg/ml). The E-Plates were continuously monitored on an RTCA system for 120 h at 37 °C with 5% CO_2. The proliferation of examined cells was monitored every 30 min and a time-dependent cell index (CI) graph was produced by the device using the RTCA software program of the manufacturer. The baseline cell index for molecules treated cells compared to cancer and control cells was calculated for at least two measurements from three independent experiments.

Total RNA isolation and cDNA synthesis

The cells were plated at a density of 5×10^5 cells in a 6-well plate with a 2-mL culture medium. After keeping the drug-loaded *C. libani* and *P. nigra* sporopollenin for 24 h. in the cell culture of CaCo-2 and Vero, the cells were washed twice with PBS, and total RNA was isolated with Trizol Reagent. 1 μg RNA was reverse transcribed by oligo(dT) primers with Transcriptor High Fidelity cDNA Synthesis Kit (EUX, Germany) according to the manufacturer's instructions.

Quantitative real-time RT-PCR

Quantitative real-time RT-PCR analysis was performed using a Lightycycler 480 (Roche, Germany). Complementary DNA (10 ng), 2.1 μL of PCR-grade water, 5 μL of SYBR Green real-time PCR master mix, and 1.5 μL of primer pairs were mixed in a PCR tube. PCR was performed with an initial denaturation at 95 °C for 10 s, followed by amplification for 40 cycles, each cycle consisting of denaturation at 95 °C for 5 s, annealing at 65 °C for 60 s. The primers are shown in Table 1. The housekeeping gene, GAPDH, was used for normalization. The qRT-PCR experiments were repeated three times. The $2^{-\Delta\Delta CT}$ method was used to calculate the fold change of mRNA expression level. To validate the size of amplified fragments, PCR products were separated by electrophoresis through 2.0% agarose gels and visualized with ethidium bromide.

Table 1 Sequences of forward (_F) and reverse (_R) primers (5′→3′) of *FOXO3* and *MYC* genes	*FOXO3*_F	TGAATGATGGGCTGACTGAA
	*FOXO3*_R	CTGGCGTAGGGAGTTCAGAG
	*MYC*_F	AGCAGAGGAGCAAAAGCTCA
	*MYC*_R	ACTCAGCCAAGGTTGTGAGG
	*GAPDH*_F	CGACCACTTTGTCAAGCTCA
	*GAPDH*_R	AGGGGAGATTCAGTGTGGTG

Results and discussions

FT-IR

FT-IR analysis was carried out to investigate the chemical interactions between sporopollenin and drug. FT-IR spectra of *OX*, *CD*, *CD-SP*, *CD-SP-OX*, *PN*, *PN-SP,* and *PN-SP-OX* are given in Fig. 1. In the spectrum of OX, the peaks observed at 3211.3 cm^{-1} and 3160.1 cm^{-1} were ascribed to N–H bonding. The sharp peak at 1696.3 cm^{-1} corresponds to the stretching vibrations of the carbonyl groups (C=O) of *OX*. The N–H bending peak was observed at 1609.7 and 807.82 cm^{-1}. We also observed that the FT-IR spectra of both raw pollens, i.e., *CD* and *PN* were similar. The broad peaks were observed at about 3345 cm^{-1} due to the intermolecular O–H bonding in the FT-IR spectra of raw pollens (*CD* and *PN*). Amide I and amide II linkages of the protein structure of raw pollens have appeared at 1605 and 1515 cm^{-1} for both pollens. The stretching peaks of the sugar rings of polysaccharides in raw
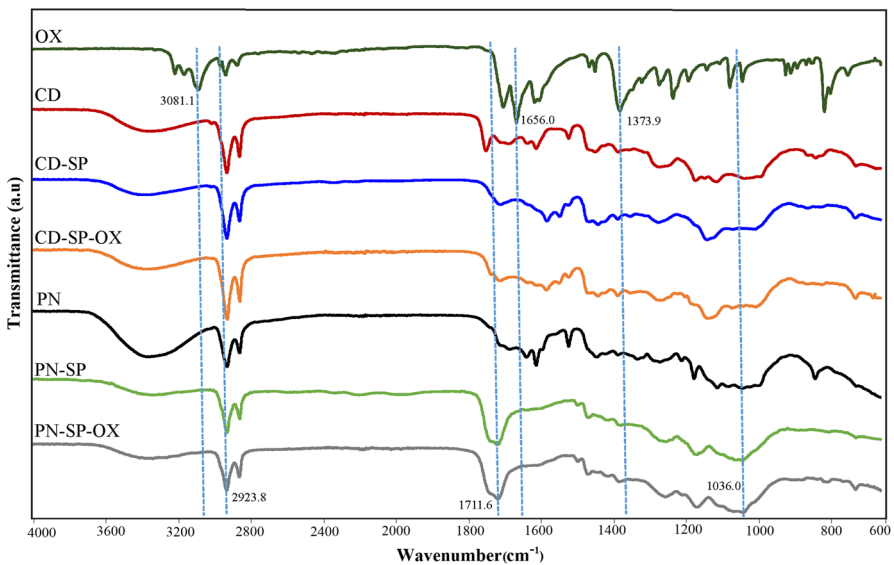

Fig. 1 FT-IR spectra of Oxaliplatin drug (*OX), Cedrus libani* raw pollen (*CD*), *Cedrus libani* sporopollenin (*CD-SP*), Oxaliplatin loaded *Cedrus libani* Sporopollenin (*CD-SP-OX*), *Pinus nigra* raw pollen (PN), *Pinus nigra* sporopollenin (*PN-SP*) and Oxaliplatin loaded *Pinus nigra* sporopollenin (*PN-SP-OX*)

pollens were recorded as the broad peaks between the 1100-1028 cm^{-1} for *CD* and *PN*.

Although the certain chemical structure of sporopollenin has not been explained until today, some research groups have been identified unsaturated fatty acids, olefinic, and aromatic functional groups found in the sporopollenin [6]. The authors determined that sporopollenin which consists of C, H, and O is an organic polymer and is nitrogen-free [8, 44]. The chemical structure of sporopollenin can be different by species [44]. In the present study, the FT-IR spectra of CD-SP and PN-SP showed that the chemical structures of the extracted sporopollenin's are different from *CD* and *PN*. When compared the *CD* spectrum with the FT-IR spectrum of the CD-SP, the new peaks were observed at 1575.6 and 1538.9 cm^{-1} due to the sporopollenin polysaccharide structures. In the PN-SP spectrum, the O–H bonding peak was shifted to 3325.2 cm^{-1} and the intensity of the peak decreased. However, a sharp peak appeared at 1713.4 cm^{-1} due to the olefinic acid structures. In the *CD-SP-OX* spectrum, it was seen that the C–H stretching of *CD-SP* shifted to higher wavenumber due to the effect of the C-H stretching of drug molecules. N–H bending vibrations of Oxaliplatin was observed at 1603.6 cm^{-1}. Alkane C–H bending of *OX* and C–H bending of *CD-SP* were overlapped and intensified at 1378.3 cm^{-1}. In the *PN-SP-OX* spectrum, the O–H band was becoming broader due to the effect of the N–H bending of *OX*. The peaks in the region of 1245–1500 cm^{-1} were intensified because of the drug molecules. These results were showed that the drug was successfully loaded into *CD-SP* and *PN-SP*.

Scanning electron microscopy (SEM) and light microscopy analysis

SEM analysis was carried out to evaluate the pollen and sporopollenin structures and to better understand the drug loading mechanism. *C. libani* and *P. nigra* have monad pollens consisting of two pollen saccus which are connected to the main body called Corpus at the distal pole called Corpus. The main body of the pollen is surrounded by two wall layers, intin and exin. The pollen saccus is alveolar vesicles, which consist of exine (Figs. 2c, g and 3b, f). As is known that sporopollenin isolation consists of two steps, i.e., acid hydrolysis and base hydrolysis for the removal of internal proteins and pigment structures. The same procedure was followed for the production of *CD-SP* and *PN-SP*. SEM micrographs confirmed the successful isolation of sporopollenin. Compared to the untreated pollens, the porous surface becomes visible after the removal of organic compounds through acid and base treatments. SEM micrographs revealed that acid treatment leads to the structural disintegration of sporopollenin. Following the acid hydrolysis treatment, *CD* preserves its structural integrity to a large extent (85–90%), and transformed into sporopollenin capsules (cages) only with a small cleavage on the leptoma (Figs. 2d and 3g). In the case of *PN*, the acid hydrolysis resulted in a complete structural disintegration (90–95%) and form sporopollenin sheets like structures or plaques. Only a small percentage (5–10%) of the pollens retained their original shape (cages), leaving only a cleavage on the leptoma (Figs. 2h and 3c). Although the acid hydrolysis resulted in the structural deformation of *PN-SP*, the sporopollenin was porous which could be
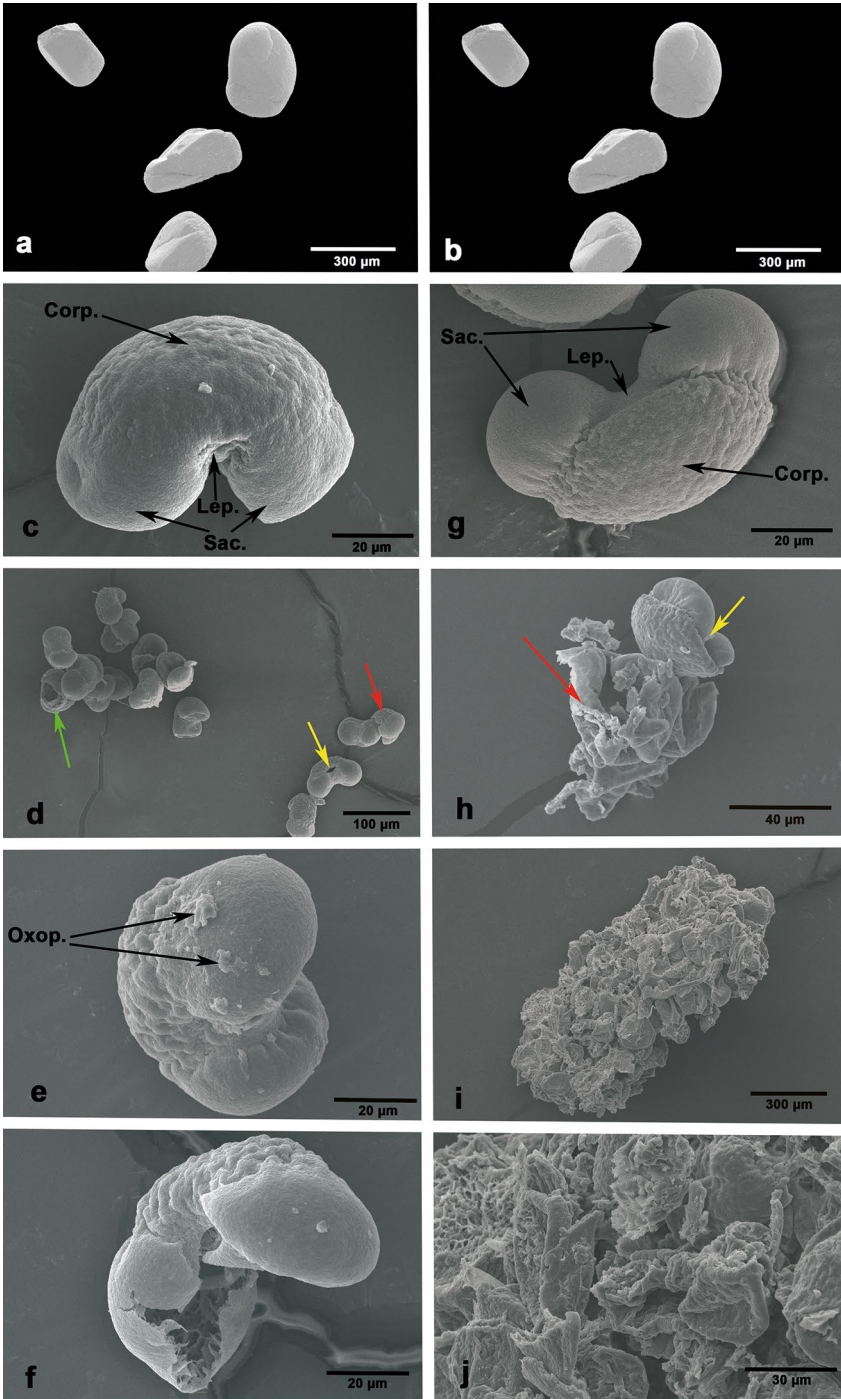
Fig. 2 SEM images of **a**, **b** Oxaliplatin drug (*OX*); **c** *Cedrus libani* raw pollen (*CD*); **d** *Cedrus libani* spo- ▶ ropollenin (*CD-SP*); **e**, **f** Oxaliplatin loaded *Cedrus libani* Sporopollenin (*CD-SP-OX*); **g** *Pinus nigra* raw pollen (PN); **h** *Pinus nigra* sporopollenin (*PN-SP*) and **i**, **j** Oxaliplatin loaded *Pinus nigra* sporopollenin (*PN-SP-OX*). (The red arrow shows the sporopollenin plaques, the yellow arrows indicate the capsules of the sporopollenin split from the leptoma region, the green arrow shows the capsules of the sporopollenin split from the saccus region) (color figure online)

help trap or adsorb the Oxaliplatin particles on its surface (Fig. 2d, h). In the current study, a commonly known anticancer drug Oxaliplatin was applied in the form of a water solution. Considering the cumulative control release and drug encapsulation results showing, it can be assumed that the drug has been encapsulated into *CD-SP* by adsorption or direct penetration through porous walls (Figs. 2e, f and 3h). *PN*, which were highly decomposed into sporopollenin plaques, form big granules together with Oxaliplatin solution (Figs. 2i, j and 3d).

In the release tests, *PN-SP-OX* has initially released 35–40% of the drug while *CD-SP-OX* revealed a 15–20% release in the first 4 h. As is clear from SEM images that acid hydrolysis of *CD* retained its structural integrity to a large extent (85–90%) compared to *PN*. SEM images of *CD-SP-OX* have revealed very little superficial Oxaliplatin residues after the encapsulation. This confirmed that the loaded drug to *CD-SP* has been encapsulated inside or adsorbed on the surface of the cages. On the other hand, as evident from SEM micrographs, following the acid treatment, the pollens of *P. nigra* lost its structural integrity (90–95%) and form sporopollenin plaques. The drug loaded to these sporopollenin plaques was adsorbed on the surface and some drug particles remain on the surface and acted as adhesive for other plaques leading to the formation of granule like structures. The drug particles trapped between the sporopollenin plaques and those present superficially released quickly into the media followed by slow release from sporopollenin cages and adsorbed on the walls. These phenomena also explained the initial release in 4 h by *CD-SP-OX* and *PN-SP-OX*.

Thermogravimetric analysis (TGA)

TGA was carried out to evaluate the thermal stabilities of the pollens and drug-loaded sporopollenin. The obtained thermograms of *PN* and *CD*, *PN-SP*, *CD-SP*, *OX*, *PN-SP-OX,* and *CD-SP-OX* are given in Fig. 4. The TG curves revealed that Oxaliplatin has been degraded at 270–330 °C (Maximum degradation 283 °C). Oxaliplatin has been reported to be thermally degraded at approximately 300° C in previous studies [45, 49]. During this degradation, elements like C, H, O, N were completely degraded, leaving only platin residues. The metal residue for Oxaliplatin after TGA degradation was recorded as 46.74% (Fig. 4a). When the percent platin content of Oxaliplatin was calculated, it was recorded as approximately 49.10% and this value was close to the platin residue recorded during thermal degradation. Five different decomposition stages were recorded for the *PN* and *PN-SP* (Figs. 4b, 5a). The initial mass loss in the thermograms of all the tested samples is attributed to the evaporation of adsorbed structural water molecules [37]. The second, third, and fourth mass loss can be attributed to
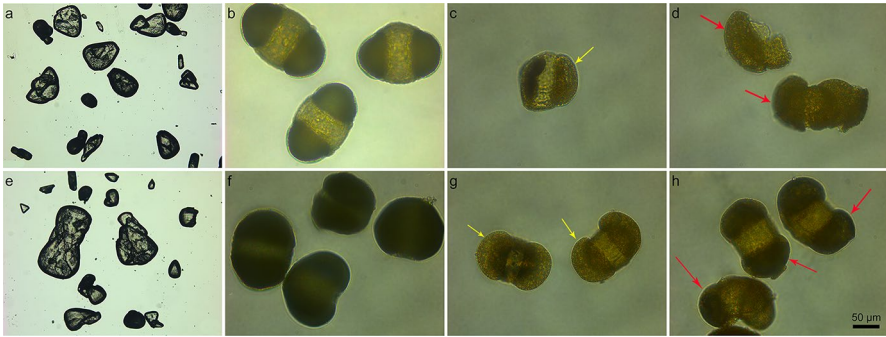
Fig. 3 Light microscopy images of **a**, **e** Oxaliplatin drug (*OX),* **b** *Pinus nigra* raw pollen (PN), **c** *Pinus nigra* sporopollenin (*PN-SP*), **d** Oxaliplatin loaded *Pinus nigra* sporopollenin (*PN-SP-OX*), **f** *Cedrus libani* raw pollen (*CD*), **g** *Cedrus libani* sporopollenin (*CD-SP*) and **h** Oxaliplatin loaded *Cedrus libani* Sporopollenin (*CD-SP-OX*)

the degradation of pollen intine (structural materials such as cellulose, genetic material, lipid, etc.) [30]. Degradation of *PN-SP-OX* was recorded in four stages (Fig. 5c). The first decomposition up to 100° C can be attributed to the evaporation of the bound water, while the second decomposition, maximum degradation around 345° C is due to the degradation of the carbohydrates remaining in the sporopollenin structure after the removal of genetic material and pectin from pollen (*P. nigra*) structure. The higher ash content in Oxaliplatin loaded sporopollenin (24.3%) is due to the platin residue, a structural component of Oxaliplatin. The thermograms of *CD* revealed the thermal degradation in four steps (Fig. 4c). The first mass loss around 53.1 °C, can be ascribed to the evaporation of structural water molecules. The second and third mass losses have occurred at 250 and 380 °C displaying a big difference. This mass loss is probably caused by the degradation of pectin and cellulose [46]. The maximum thermal decomposition temperatures for pectin and cellulose are 262.8° C and 378.9° C, respectively. The sharp decomposition at 432.5 °C may be due to partial depolymerization and disintegration of the sporopollenin wall. For *CD-SP*, three separate degradations were observed (Fig. 5b). After the addition of Oxaliplatin (*CD-SP-OX*), the mass loss in the second degradation increased from 37.8 to 41.5% (Fig. 5d). The maximum degradation of sporopollenin was achieved at approximately 440 °C (Table 2). It is thought that the mass loss occurring around 400–650 °C is caused by the deterioration of the wall (exine) of sporopollenin. According to these results, sporopollenin has high thermal stability. Furthermore, it shows that the normal thermal properties of Oxaliplatin change after incorporation Oxaliplatin into sporopollenin samples and that Oxaliplatin has high decomposition temperatures. The higher the thermal decomposition temperature, the higher the thermal stability has been noted in previous studies [22, 23, 50]. Mujtaba et al. [24] reported that *P. orientalis* sporopollenin has higher thermal stability than biopolymers such as cellulose and chitin [24]. Compared to the results of the current study, it was observed that *P. nigra* and *C. libani* sporopollenin have high
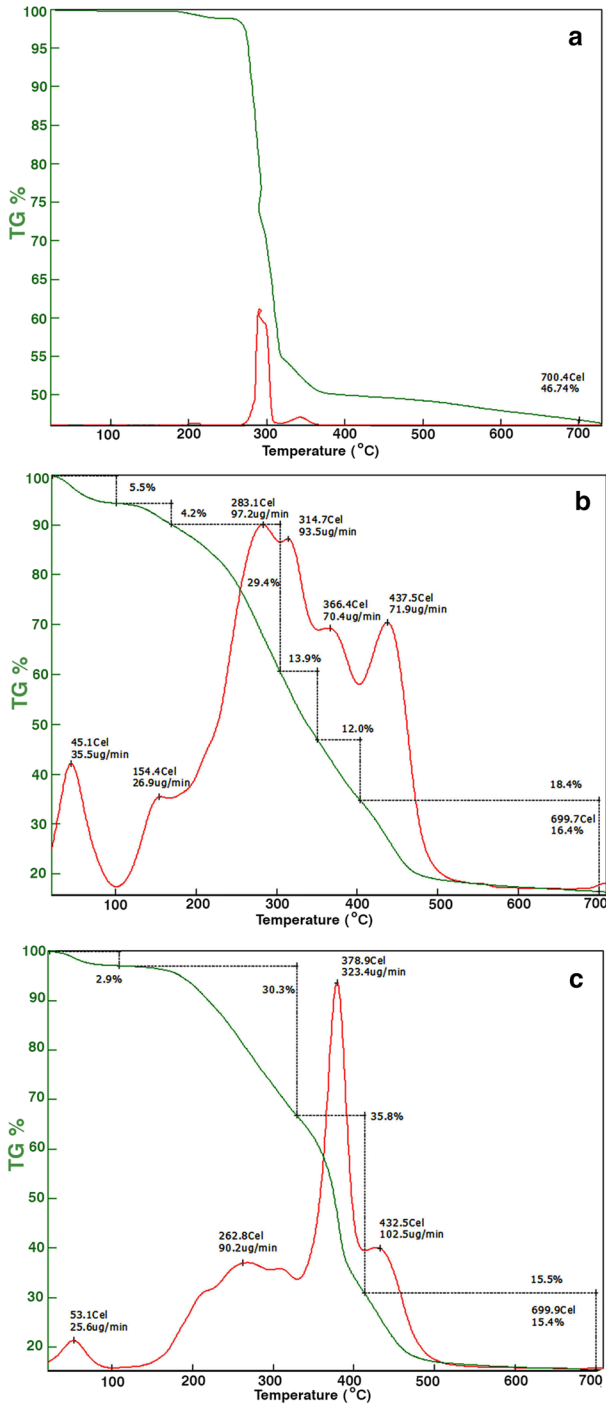
Fig. 4 TGA and DTG curves: **a** Oxaliplatin drug *(OX)*, **b** *Pinus nigra* raw pollen *(PN)*, **c** *Cedrus libani* raw pollen *(CD)*
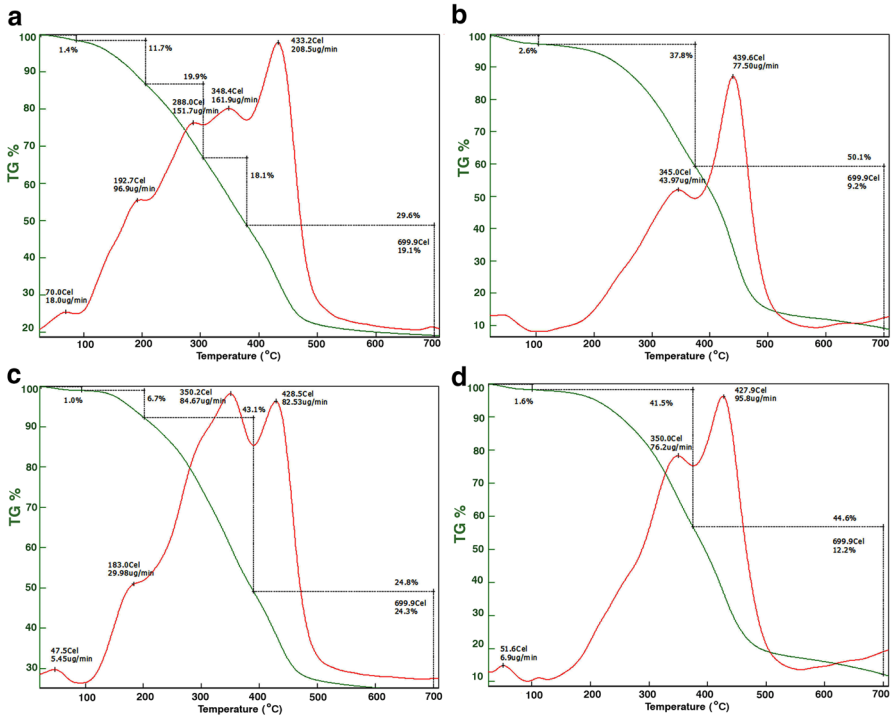
Fig. 5 **a** *Pinus nigra* sporopollenin (*PN-SP*), **b** *Cedrus libani* sporopollenin (*CD-SP*) **c** Oxaliplatin loaded *Pinus nigra* sporopollenin (*PN-SP-OX*), and **d** Oxaliplatin loaded *Cedrus libani* Sporopollenin (*CD-SP-OX*)

Table 2 Detailed thermogravimetric degradation peaks of Oxaliplatin drug (*OX*), *Pinus nigra* raw pollen (PN), *Pinus nigra* sporopollenin (*PN-SP*), Oxaliplatin loaded *Pinus nigra* sporopollenin (*PN-SP-OX*), *Cedrus libani* raw pollen (*CD*), *Cedrus libani* sporopollenin (*CD-SP*) and Oxaliplatin loaded *Cedrus libani* Sporopollenin (*CD-SP-OX*)

Samples	Degradation peaks (°C)				
OX	283	–	–	–	–
PN	45.1	283.1	314.7	366.4	437.5
PN-SP	70.0	192.7	288.0	348.4	433.2
PN-SP-OX	47.5	183.0	350.2	428.5	–
CD	53.1	262.8	378.9	432.5	–
CD-SP	55.3	345.0	439.6	–	–
CD-SP-OX	51.6	350.0	427.9	–	–

dTGmax temperature and this sporopollenin has more stable structures. In this study, the TGA results of *P. nigra* and *C. libani* species did not show a significant difference in terms of thermal stability.

Encapsulation efficiency

The encapsulation efficiency (%) of *CD* and *PN* was recorded as 10.06% and 38.62% respectively. An important difference was observed among the encapsulation % of the two pollens. Here in the current study, a passive drug loading technique was adopted for the Oxaliplatin encapsulation into *CD* and *PN*. The variance in the encapsulation percentages can be attributed to the structural modifications during the isolation. As discussed in detail in the SEM section, acid treatment of *PN* leads to major structural disintegration resulting in sporopollenin plaques formation providing a larger surface area for the drug to interact and penetrate. Due to the enhanced surface area, a large amount (38.63%) of Oxaliplatin has been adsorbed into the sporopollenin porous surface. On the other hand, the *CD* preserved its structural integrity up to a large extent during the isolation, thus resulting in sporopollenin cages. As passive loading techniques do not involve any active external forces [25] for loading the drug inside the sporopollenin cages, the loading efficiency of *CD* was recorded lower as compared to *PN*.

It is known that the morphologies of pollen grains vary according to the species. The sporopollenen, generally has a large internal space, pore, reticulated or flat surface, uniform size and is highly biocompatible. The uniformity in size is specific specie property and shows significant variation from specie to specie. Different surface morphologies may also vary in different usage areas of sporopollens. In a study, it has been shown that *P. orientalis* sporopollenen has a porous and reticulated surface and this surface has a good drug encapsulation ability. In addition, it was determined that not only the surface but also the drug loading technique had an effect on the encapsulation efficiency [24]. The sporopollenin of Phoenix *dactylifera L.* sporopolenes have also been reported to increase the encapsulation efficiency due to macroporous surface morphology [3]. In the same regard in current study, sporopollenin from different species have different morphologies in terms of pore size, number of pores and overall size. These difference size and pores significantly effected the encapsulation and release of encapsulated drug.

Drug release measured in simulated pH solutions

In vitro release studies of the Oxaliplatin *(OX)* and Oxaliplatin loaded *P. nigra* (*PN-SP-OX*) and *C. libani* sporopollenin (*CD-SP-OX*) were performed in PBS (pH 7.4) and results are presented in Fig. 6. The release profile of the *OX* revealed an initial fast release during the first 4 h and then dramatically decreased. Overall drug-loaded sporopollenin has shown a slower release rate than the pure drug. The reason behind this slow release can be due to the successful entrapment of the drug inside of the sporopollenin microcapsules and sporopollenin plaques of *P. nigra*. Oxaliplatin was completely dissolute in PBS for 4 h, whereas in the same time frame, the cumulative releases of Oxaliplatin from *CD-SP-OX* and *PN-SP-OX* were recorded as 15.72% and 28.97% respectively. This fluctuation in the initial release values is attributed to the structural changes (sporopollenin plaques formation) that occurred during the *P. nigra* sporopollenin extraction process (Better explained in SEM section). The
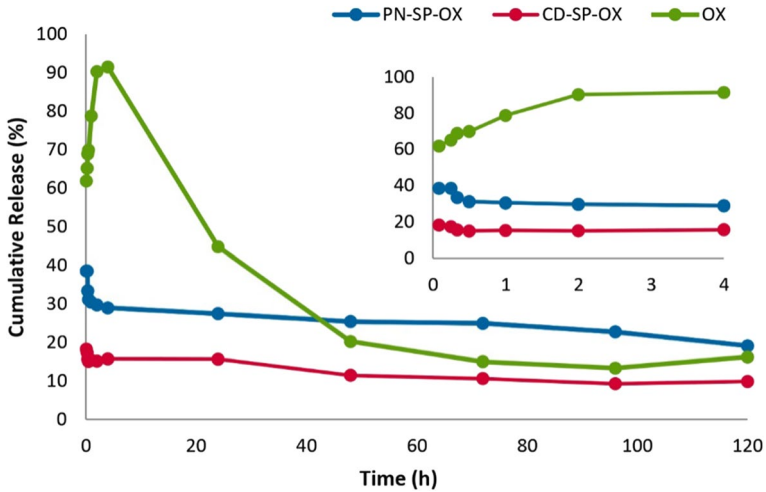
Fig. 6 Release properties of sporopollenin microcages from *Cedrus libani* and *Pinus nigra* via passive loading technique in PBS solution

results were also found in agreement with the cell studies conducted for checking the release effect in real time using a real-time cell analyzer (xCELLigence). Also, chitosan nanoparticles [42] and immune-hybrid nanoparticles [39] were used as drug delivery systems for Oxaliplatin in the literature. The Oxaliplatin release from chitosan nanoparticles was found to be under 20% for the first 8 h in the Vivek et al. study [42]. Tummala et al. [39] reported that the Oxaliplatin release from immune-hybrid nanoparticles showed a biphasic pattern of drug release in pH = 7.4. The authors explained that the cause of the initial burst release was unentrapped drug molecules. However, the initial burst release did not observe in the present study. The reason for this result can be due to the entrapment of the drug molecules into the sporopollenin cages and plaques. Consequently, the results of the present in vitro release study demonstrated that the *PN-SP* and *CD-SP* could be used as a drug carrier.

Drug release measured via the xCELLigence RTCA system

In the current study, xCELLigence a real-time cell analyzer (RTCA) system was used to determine the slow release activity of *P. nigra* and *C. libani* sporopollenin in CaCo-2 and Vero cells in real time (Fig. 7). Although traditional drug release and cytotoxic assays are performing well, it is time to support them through advancing technologies of the field. RTCA system monitors cell growth by measuring electrical impedance, which is represented as a cell index. xCELLigence detects and measures the phenotypic changes occurring in the cells as a result of the released drug from the sporopollenin through gold microelectrodes mounted at the bottom of the system-specific plates. The prolonged cell proliferation activity reflects the slow
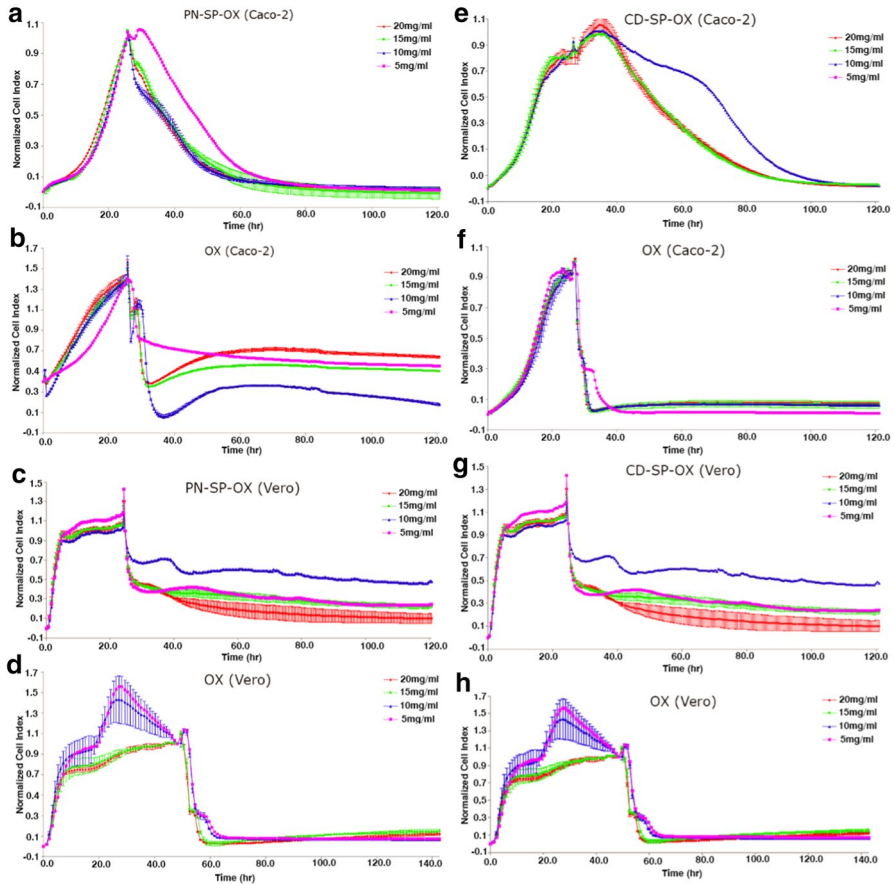
Fig. 7 Cell proliferation assay of Caco-2 and Vero cell lines was conducted in the presence of free Oxaliplatin and Sporopollenin loaded with Oxaliplatin using the xCELLigence system. **a** sporopollenin of Oxaliplatin loaded *Pinus nigra* sporopollenin/CaCo-2; **b** free Oxaliplatin/CaCo-2; **c** sporopollenin of Oxaliplatin loaded *Pinus nigra* sporopollenin/Vero, **d** free Oxaliplatin/Vero; **e** sporopollenin of Oxaliplatin loaded *Cedrus libani* sporopollenin/CaCo-2; **f** free Oxaliplatin/CaCo-2; **g** sporopollenin of Oxaliplatin loaded *Cedrus libani* sporopollenin/Vero; **h** free Oxaliplatin/Vero. (pink line: 5 mg/ml; blue line: 10 mg/ml; green line: 15 mg/ml; red line: 20 mg/ml). (The prolonged cell proliferation activity reflects the slow release ratio of Oxaliplatin from *Pinus nigra* and *Cedrus libani* in Caco-2 cells and displayed as normalized cell index by the xCELLigence) (color figure online)

release ratio of Oxaliplatin from *PN-SP-OX* and *CD-SP-OX* in Caco-2 and Vero cells and was calculated as normalized cell index by the xCELLigence.

CD-SP-OX and *PN-SP-OX* caused cytotoxicity at three doses (5, 10, 15 mg/ml). The IC$_{50}$ values of *PN-SP-OX* were calculated as 10 mg/ml and 14.62 mg/ml for CaCo-2 and Vero cell lines, respectively. The IC$_{50}$ values for *CD-SP-OX* were determined to 5 mg/ml for both examined cell lines. The observed cell index value referred that *CD-SP-OX* and *PN-SP-OX*-mediated slow release of Oxaliplatin significantly induced the cell index in a dose-dependent manner on Caco-2 cell compared

to Vero cells for over 120 h incubation time (Fig. 6a–h). A prolonged-release pattern was observed for *CD-SP-OX* and *PN-SP-OX* compared to free Oxaliplatin drug, with an IC_{50} value of 5 and 14.62 mg/ml after 120 h incubation time. Oxaliplatin displayed an antiproliferative effect in CaCo-2 cells at approximately 5 h at all concentrations, while *PN-SP-OX* revealed a long-delivery effect on CaCo-2 cancer cells for about 41 h. *PN-SP-OX* showed about an 8 times longer release effect than the control drug (free Oxaliplatin). Interestingly, *PN-SP-OX* applied at the concentration of 10 mg/ml displayed a lower antiproliferative effect on Vero normal cells providing a clue that the slow release of the therapeutics also minimizes the harmful effects on the normal healthy cells (Fig. 7a–d). In the case of *CD-SP-OX*, at the concentration of 5 mg/ml, *a* prolonged proliferation effect on CaCo-2 cell was observed, which lasts for 45 h. At the same concentration, the free Oxaliplatin showed a 5 h antiproliferation activity. Besides, slow release activity from *CD-SP-OX* was observed in Vero cells (Fig. 7e–h).

Considering the overall results, it can be stated that sporopollenin-mediated slow release revealed a prolonged and slow release of Oxaliplatin in both CaCo-2 and Vero cells. However, the slow release in healthy cells decreases the antiproliferative effect as a result of the loaded therapeutic i.e., Oxaliplatin. The use of RTCA gives an idea about the beneficial effect of slow release of Oxaliplatin on healthy cells.

Expression of *FOXO3* and *MYS*

To better understand the apoptosis effects of sporopollenin-mediated slow release of Oxaliplatin on cancer (CaCo-2) and healthy cells (Vero), the expression profiles of two reference genes for apoptosis were investigated using a qRT-PCR. *FOXO3* and *MYS* genes were selected for this purpose as they are thought to be responsible for controlling key pathways during cell apoptosis (detailed functions of both genes have been described in the "Introduction" section).

As shown in Fig. 8, a 20-fold increase was recorded for the *FOXO3* mRNA expression in the CaCo-2 cell line when treated with PN-SP-OX ($p < 0.05$) (Fig. 7a). Interestingly, in the case of Vero cells, no significant increase was recorded in the expression of FOXO3 after treating it with PN-SP-OX (Fig. 7b) ($p < 0.05$). The level of *MYC* gene expression decreased approximately twofold on the CaCo-2 cell compared to the control (Fig. 7c). In Vero normal cell, the expression level of the *MYC* gene decreased about 8 times compared to control ($p < 0.05$) (Fig. 7d). In the case of CD-SP-OX, the level of *FOXO3* gene expression on the CaCo-2 cell increased by about 36-fold compared to the control but a decrease of twofold was detected in the Vero cell ($p < 0.05$) (Fig. 7e, f). *MYC* gene expression of CD-SP-OX was not statistically significant compared to the control (OX) but increased gene expression compared to the control of CaCo-2 cells (Fig. 7g). The same material showed a threefold decrease in *MYC* gene expression in Vero cell ($p < 0.05$) (Fig. 7h). In summary, the expression of MYC and *FOXO-3* genes was increased in CaCo2 cells and decreased non-cancerous Vero cells. The results demonstrated that the increased expression level of these gene-induced apoptosis. The slow release of anticancer drugs in tumor cells may lead to the development of important and novel strategies based on slow release in the treatment of
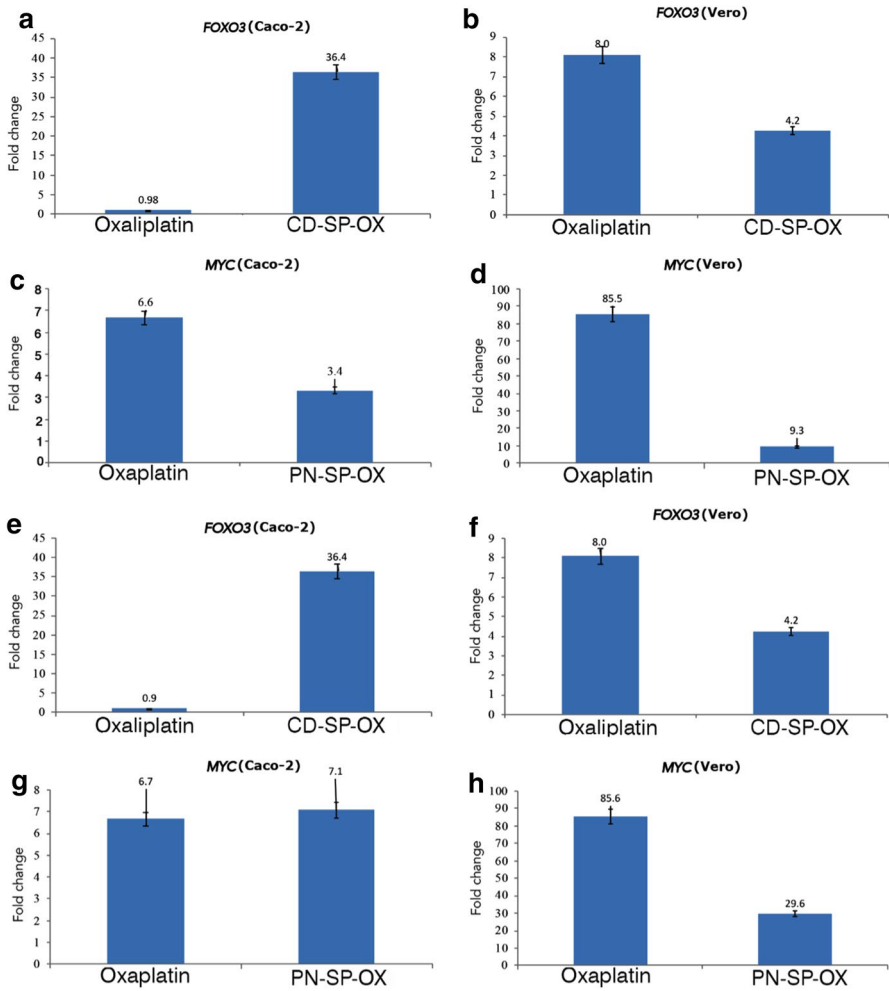
Fig. 8 Expression profiles of FOXO3 and MYC genes in Caco-2 and Vero cells treated with Oxaliplatin (OX) and Oxaliplatin loaded Sporopollenin

cancer. However, considering the current clue given by this study a more detailed study is needed to investigate the apoptosis linkage with the slow release on the protein level.

Conclusion

Sporopollenin exine capsules (SECs) extracted from plant pollens have successfully established its position in the category of biomaterials for control release applications, thanks to its robust structural and morphological features making it an ideal vehicle for encapsulation and control release of drugs. Considering the results of the current study, it can be stated that the sporopollenin of *C. libani* and *P. nigra*

successfully demonstrated slow release abilities of the Oxaliplatin (40–45 h). The sporopollenin-mediated extended-release of Oxaliplatin can overcome the negative effect of the routine used cancer drugs. Both the in vitro release assay in PBS and CaCo-2 and Vero cell cultures assay in real-time cell analyzer (xCELLigenece) had confirmed the slow release by sporopollenin of *C. libani* and *P. nigra*. Apoptosis plays a critical role in tumorigenesis, in this study, we have provided an understanding of the linkage of sporopollenin aided slow release and apoptosis mechanisms by checking the expression levels of *MYC* and *FOXO-3* genes. However, further investigation of other genes related apoptosis pathway is required to advance the results of the present study.

Availability of data and material Not applicable.

Code availability Not applicable.

Compliance with ethical standards

Conflict of interest The authors declare that they have no conflict of interest.

Ethics approval Not applicable.

References

1. Agrawal M et al. (2020) Recent strategies and advances in the fabrication of nano lipid carriers and their application towards brain targeting. Journal of Controlled Release
2. Alan Ş, Yıldırım Ö, Pınar N, Seçil D, Keçeli T, Çeter T, Mısırlıgil Z (2009) Betula pendula Roth (syn = B. verrucosa) polenine duyarlı hastalarda IgE reaktivite profilleri. Asthma Allergy Immunol 7:100–105
3. Alshehri SM, Al-Lohedan HA, Al-Farraj E, Alhokbany N, Chaudhary AA, Ahamad T (2016) Macroporous natural capsules extracted from *Phoenix dactylifera* L. spore and their application in oral drugs delivery. Int J Pharm 504:39–47
4. Brown JM, Attardi LD (2005) The role of apoptosis in cancer development and treatment response. Nat Rev Cancer 5:231–237
5. Caminade A-M, Turrin C-O (2014) Dendrimers for drug delivery. J Mater Chem B 2:4055–4066
6. Diego-Taboada A, Beckett S, Atkin S, Mackenzie G (2014) Hollow pollen shells to enhance drug delivery. Pharmaceutics 6:80–96
7. Diego-Taboada A et al (2013) Protein free microcapsules obtained from plant spores as a model for drug delivery: ibuprofen encapsulation, release and taste masking. J Mater Chem B 1:707–713
8. Domínguez E, Mercado JA, Quesada MA, Heredia A (1999) Pollen sporopollenin: degradation and structural elucidation. Sex Plant Reprod 12:171–178
9. Du WW, Fang L, Yang W, Wu N, Awan FM, Yang Z, Yang BB (2017) Induction of tumor apoptosis through a circular RNA enhancing Foxo3 activity. Cell Death Differ 24:357–370

10. Duro-Castano A, Talelli M, Rodríguez-Escalona G, Vicent M (2019) Smart polymeric nanocarriers for drug delivery. In: Smart polymers and their applications. Elsevier, pp 439–479
11. Fan T-F et al (2020) Degradation of the sporopollenin exine capsules (SECs) in human plasma. Appl Mater Today 19:100594. https://doi.org/10.1016/j.apmt.2020.100594
12. Fan T et al (2018) Extraction of cage-like sporopollenin exine capsules from dandelion pollen grains. Sci Rep 8:1–11
13. Kumar A, Montemagno C, Choi H-J (2017) Smart microparticles with a pH-responsive macropore for targeted oral drug delivery. Sci Rep 7:1–15
14. Li W et al (2019) AuNPs as an important inorganic nanoparticle applied in drug carrier systems. Artif Cells Nanomed Biotechnol 47:4222–4233
15. Madaan K, Kumar S, Poonia N, Lather V, Pandita D (2014) Dendrimers in drug delivery and targeting: drug-dendrimer interactions and toxicity issues. J Pharm Bioallied Sci 6:139
16. Mir SH, Hasan P, Danish EY, Aslam M (2020) Pd-induced phase separation in poly (methyl methacrylate) telopolymer: synthesis of nanostructured catalytic Pd nanorods. Colloid Polym Sci 1–8
17. Mir SH, Nagahara LA, Thundat T, Mokarian-Tabari P, Furukawa H, Khosla A (2018) Organic-inorganic hybrid functional materials: an integrated platform for applied technologies. J Electrochem Soc 165:B3137
18. Mir SH, Ochiai B (2016) Development of hierarchical polymer@ Pd nanowire-network: synthesis and application as highly active recyclable catalyst and printable conductive ink. ChemistryOpen 5:213–218
19. Mir SH, Ochiai B (2016) Fabrication of polymer-Ag honeycomb hybrid film by metal complexation induced phase separation at the air/water interface. Macromol Mater Eng 301:1026–1031
20. Mir SH, Ochiai B (2017) One-pot fabrication of hollow polymer@ Ag nanospheres for printable translucent conductive coatings. Adv Mater Interfaces 4:1601198
21. Mir SH, Ochiai B (2018) Conductive polymer-Ag honeycomb thin film: the factors affecting the complexity of the microstructure. J Electrochem Soc 165:B3030
22. Mujtaba M, Murat K, Ceter T (2018) Differentiation of thermal properties of pollens on genus level. Commun Fac Sci Univ Ankara Ser C Biol 27:177–184
23. Mujtaba M, Murat K, Ceter T (2018) An investigation of pollen grain thermal diversity on species level. Commun Fac Sci Univ Ankara Ser C Biol 27:170–176
24. Mujtaba M, Sargin I, Akyuz L, Ceter T, Kaya M (2017) Newly isolated sporopollenin microcages from Platanus orientalis pollens as a vehicle for controlled drug delivery. Mater Sci Eng, C 77:263–270. https://doi.org/10.1016/j.msec.2017.02.176
25. Mundargi RC, Tan E-L, Seo J, Cho N-J (2016) Encapsulation and controlled release formulations of 5-fluorouracil from natural Lycopodium clavatum spores. J Ind Eng Chem 36:102–108
26. O'Donnell KA, Wentzel EA, Zeller KI, Dang CV, Mendell JT (2005) c-Myc-regulated microRNAs modulate E2F1 expression. Nature 435:839–843
27. Paunov VN, Mackenzie G, Stoyanov SD (2007) Sporopollenin micro-reactors for in situ preparation, encapsulation and targeted delivery of active components. J Mater Chem 17:609–612
28. Pomelli CS, D'Andrea F, Mezzetta A, Guazzelli L (2020) Exploiting pollen and sporopollenin for the sustainable production of microstructures. N J Chem
29. Sargin I et al (2017) Controlled release and anti-proliferative effect of imatinib mesylate loaded sporopollenin microcapsules extracted from pollens of Betula pendula. Int J Biol Macromol 105:749–756
30. Sargın İ, Arslan G (2015) Chitosan/sporopollenin microcapsules: preparation, characterisation and application in heavy metal removal. Int J Biol Macromol 75:230–238
31. Shen Y et al (2010) Prodrugs forming high drug loading multifunctional nanocapsules for intracellular cancer drug delivery. J Am Chem Soc 132:4259–4265
32. Simpson MG (2019) Plant systematics. Academic Press, London
33. Sin A, Pınar N, Mısırlıgil Z, Çeter T, Yıldız A, Alan Ş (2007) Polen Allerjisi (Türkiye Allerjik Bitkilerine Genel Bir Bakış) Ankara: Engin Yayınevi
34. Soppimath KS, Aminabhavi TM, Kulkarni AR, Rudzinski WE (2001) Biodegradable polymeric nanoparticles as drug delivery devices. J Controlled Release 70:1–20
35. Stella B, Andreana I, Zonari D, Arpicco S (2019) Pentamidine-loaded Lipid and Polymer Nanocarriers as Tunable Anticancer Drug Delivery Systems. J Pharm Sci
36. Taylor RC, Cullen SP, Martin SJ (2008) Apoptosis: controlled demolition at the cellular level Nature reviews. Mol Cell Biol 9:231–241
37. Tirkistani FA (1998) Thermal analysis of some chitosan Schiff bases. Polym Degrad Stabil 60:67–70

38. Tong R, Cheng J (2008) Paclitaxel-initiated, controlled polymerization of lactide for the formulation of polymeric nanoparticulate delivery vehicles. Angew Chem Int Ed 47:4830–4834

39. Tummala S, Gowthamarajan K, Satish Kumar M, Wadhwani A (2016) Oxaliplatin immuno hybrid nanoparticles for active targeting: an approach for enhanced apoptotic activity and drug delivery to colorectal tumors. Drug Deliv 23:1773–1787

40. Uthappa U, Kurkuri MD, Kigga M (2019) Nanotechnology advances for the development of various drug carriers. In: Nanobiotechnology in bioformulations. Springer, Berlin, pp 187–224

41. Vader P, Mol EA, Pasterkamp G, Schiffelers RM (2016) Extracellular vesicles for drug delivery. Adv Drug Deliv Rev 106:148–156

42. Vivek R, Thangam R, Nipunbabu V, Ponraj T, Kannan S (2014) Oxaliplatin-chitosan nanoparticles induced intrinsic apoptotic signaling pathway: a "smart" drug delivery system to breast cancer cell therapy. Int J Biol Macromol 65:289–297

43. Wang Y et al (2018) Pollen-inspired microparticles with strong adhesion for drug delivery. Appl Mater Today 13:303–309

44. Watson JS et al (2007) Rapid determination of spore chemistry using thermochemolysis gas chromatography-mass spectrometry and micro-Fourier transform infrared spectroscopy. Photochem Photobiol Sci 6:689–694

45. Wu L, Man C, Wang H, Lu X, Ma Q, Cai Y, Ma W (2013) PEGylated multi-walled carbon nanotubes for encapsulation and sustained release of oxaliplatin. Pharm Res 30:412–423

46. Yang H, Yan R, Chen H, Lee DH, Zheng C (2007) Characteristics of hemicellulose, cellulose and lignin pyrolysis. Fuel 86:1781–1788

47. Yang Y et al (2019) Recent advance in polymer based microspheric systems for controlled protein and peptide delivery. Curr Med Chem 26:2285–2296

48. Yoo HS, Lee KH, Oh JE, Park TG (2000) In vitro and in vivo anti-tumor activities of nanoparticles based on doxorubicin–PLGA conjugates. J Controlled Release 68:419–431

49. Zhang D et al (2016) Preparation, characterisation and antitumour activity of β-, γ-and HP-β-cyclodextrin inclusion complexes of oxaliplatin. Spectrochim Acta Part A Mol Biomol Spectrosc 152:501–508

50. Zuluaga-Domínguez C, Serrato-Bermudez J, Quicazán M (2018) Influence of drying-related operations on microbiological, structural and physicochemical aspects for processing of bee-pollen. Eng Agric Environ Food 11:57–64